Water Hammer Modeling, Comparison between Method of Characteristics and Godunov Type Finite Volume Method

Saeed-Reza Sabbagh-Yazdi [1], Ali Abbasi[2] and Nikos E Mastorakis [3]

[1] Associate Professor of K.N. Toosi University of Technology, Department of Civil Engineering, 1346 Valiasr St. 19697 Tehran, IRAN, SYazdi@kntu.ac.ir

[2] M.Sc Graduate of K.N. Toosi University of Technology, Department of Civil Engineering, 1346 Valiasr St. 19697 Tehran, IRAN, AliAbbasi.civileng@gmail.com

[3] Military Insitutes of University Education (ASEI) Hellenic Naval Academy, Terma Chatzikyriakou, 18539,Piraues, GREECE, mastor@wseas.org

Abstract

The wave resulting from instantaneous and complete valve-closure in pressurized pipe systems propagates upstream and/or downstream in the hydraulic system. The pressure (head) and velocity of the flow (waves) are important parameters in the design of pipeline systems. Analyzing and interpreting water-hammer (unsteady flow) phenomena in a pipeline are not easy tasks. For complicated cases, the governing partial differential equations can only be solved numerically. Various numerical approaches have been introduced for pipe line transient calculations. They include The Method of Characteristics (MOC), Finite Difference (FD), Wave Plan (WP), Finite Volume (FV) and Finite Element (FE). In this paper, second-

order Finite Volume (FV) Godunov type scheme is applied for water hammer problems and the results are analyzed. The developed one-dimensional model is based on Reimann solution. The implementation of boundary conditions such as reservoirs, valves, and pipe junctions in the Godunov approach is similar to that of the method of characteristics (MOC) approach. The model is applied to two classic problems (systems consisting of a reservoir, a pipe and a valve). The second-order Godunov scheme is stable for Courant number less than or equal to unity. The minimum and maximum of the pressure waves not only are computed in close agreement with laboratory data, both also in the same period of the times.

Key Words

Water-Hammer, Unsteady Pipe Flow, Finite Volume Method, Second Order Godunov Type Reiman Solver

1 Introduction

In pressurized pipeline, flow disturbance caused by pump shutdowns, or rapid changes in valve setting, trigger a series of positive and negative pressure waves large enough to rupture pipelines or damage other hydraulic devices. Negative pressure waves can also result in cavitation, pitting and corrosion. Thus accurate modeling of water hammer events (hydraulic transient) is vital for proper design and safe operation of pressurized pipeline systems. Water quality problems can also arise due to intrusion of contaminants through cracks and joints. Water quality can be affected following a water hammer event as the biofilm on the pipe is sloughed off by large shear stresses created by the transient, and particulates may be resuspended by the strong mixing of the flow inside a pipe. The design of pipeline systems, and the prediction of water quality impacts, requires efficient mathematical models capable of accurately solving water hammer problems[10].

Various numerical approaches have been introduced for pipeline transient calculation. They include the method of characteristics (MOC), finite difference (FD), wave plan (WP), finite volume (FV), and finite element (FE). Among these methods, MOC proved to be the most popular among water hammer experts. The MOC approach transforms the water hammer partial differential equations into ordinary differential equations along characteristic lines. The integration of these ordinary differential equations

from one time step to the next requires that the value of the head and flow at the foot of each characteristic line be known. This requirement can be met by one of two approaches: (i) use the MOC-grid scheme; or (ii) use the fixed-grid MOC scheme and employ interpolation in pipes, that it is impossible to make the Courant number exactly equal to one in all pipes. This interpolation artificially modifies the wave celerity and introduces artificial damping into the solution[6]. The fixed-grid MOC is the most widely accepted procedure for solving the water hammer equations and has the attributes of being simple to code, efficient, accurate, and provides the analyst with full control over the grid selection.

Results of solving the water hammer equations by the MacCormack, Lambda, and Gabutti explicit FD schemes show that these second-order FD schemes produce better results than the first-order MOC[15].

Finite element methods (FE) are noted for their ability to: (i) use unstructured grids (meshes), (ii) provide convergence and accurate results, and (iii) provide results in any point of problem domain. Jovic (1995) used the combined method of MOC and FE for water hammer modeling in a classical system (a system consisting of a reservoir, a pipe, and a valve)[7]. Mollabashi (2002) solved the water hammer equations by finite element method and applied it to a classical system[11]. Ahmadi et al. (2004) used the finite element method for water hammer problems with complicated boundary conditions[1]. They found that finite element method results are in good agreement with MOC results. However, FE schemes increase the execution time. Thus FE schemes don't have an important privilege in 1D problems.

FV methods are widely used in the solutions of hyperbolic systems, such as gas dynamics and shallow water waves. FV methods are noted for their ability to: (i) conserve mass and momentum, (ii) provide sharp resolution of discontinuities without spurious oscillations, and (iii) use unstructured grid (mesh). The first application of the FV method to water hammer problems is due to Guinot (2002). This first-order scheme is highly similar to MOC with linear space-line interpolation.

The objectives of this article are: (1) to implement the Godunov type solution for water hammer and (2) to investigate the accuracy of this method. The article is organized as follows. First, the governing equations of water hammer are given. Second, the FV form of the governing equations is provided. Third, first- and second-order Godunov schemes for the FV fluxes are formulated. Fourth, the time integration of the equations is derived. Fifth, the schemes are tested using single pipe systems. Last, the results are summarized in the Conclusions.

2 Governing Equations

Unsteady closed conduit flow is often represented by a set of 1D hyperbolic partial differential equations[15]:

$$\frac{\partial H}{\partial t}+V\frac{\partial H}{\partial x}+\frac{a^2}{g}\frac{\partial V}{\partial x}+V\sin\theta=0 \quad \text{Continuity equation} \qquad (2.1)$$

$$\frac{\partial V}{\partial t}+V\frac{\partial V}{\partial x}+g\frac{\partial H}{\partial x}+J=0 \quad \text{Momentum equation} \qquad (2.2)$$

where t=time; x=distance along the pipe centerline; $H=H(x,t)$= piezometric head; $V=V(x,t)$=instantaneous average fluid velocity; g=gravitational acceleration; a=wavespeed; θ=the pipe slope; and J=friction force at the pipe wall.

The nonlinear convective terms $V\,\partial H/\partial x$ and $V\,\partial V/\partial x$ are included in Eqs. (2.1) and (2.2). These terms, although small for the majority of water hammer problems, are not neglected in this paper. Maintaining the convective terms in the governing equations makes the scheme applicable to a wide range of transient flow problems.

3 Formulation of Finite Volume Schemes for Water Hammer

The computational grid involves the discretization of the x axis into reaches each of which has a length Δx and the t axis into intervals each of which has a duration Δt. Node (i,n) denotes the point with coordinate $x=[i-(1/2)]\Delta x$ and $t=n\Delta t$. A quantity with a subscript i and a superscript n signifies that this quantity is evaluated at node (i,n). The ith control volume is centered at node i and extends from $i-1/2$ to $i+1/2$. That is, the ith control volume is defined by the interval $[(i-1)\Delta x, i\Delta x]$. The boundary between control volume i and control volume $i+1$ has a coordinate $i\Delta x$ and is referred to either as a control surface or a cell interface. Quantities at a cell interface are identified by subscript such as $i-1/2$ and $i+1/2$.

The Riemann-based FV solution of Eqs. (2.1) and (2.2) in the ith control volume entails the following steps: (1) the governing equations are rewritten in control volume form; (2) the fluxes at a control surface are approximated using the exact solution of the Riemann problems; and (3) a time integration to advance the solution from n to $n+1$.

Eqs. (2.1) and (2.2) can be rewritten in a matrix form as follows[15]:

$$\frac{\partial \boldsymbol{u}}{\partial t} + \boldsymbol{A}\frac{\partial \boldsymbol{u}}{\partial x} = \boldsymbol{s} \tag{3.1}$$

where $\boldsymbol{u} = \begin{pmatrix} H \\ V \end{pmatrix}$; $\boldsymbol{A} = \begin{pmatrix} V & a^2/g \\ g & V \end{pmatrix}$; and $\boldsymbol{s} = \begin{pmatrix} -\sin\theta \\ -J \end{pmatrix}$.

For hyperbolic systems in nonconservative form, Eq. (3.1) can be approximated as follows[15]:

$$\frac{\partial \boldsymbol{u}}{\partial t} + \frac{\partial \boldsymbol{f}(\boldsymbol{u})}{\partial x} = \boldsymbol{s}(\boldsymbol{u}) \tag{3.2}$$

where $f(\boldsymbol{u}) = \overline{\boldsymbol{A}}\boldsymbol{u}$; $\overline{\boldsymbol{A}} = \begin{pmatrix} \overline{V} & a^2/g \\ g & \overline{V} \end{pmatrix}$; and $\overline{V}$ =mean value of V to be specified later. Setting $\overline{V} = 0$, the scheme reverts to the classical water hammer case where the convective terms are neglected.

The mass and momentum equations for control volume i is obtained by integration Eq. (3.2) with respect to x from control surface i-1/2 to control surface i+1/2. The results is:

$$\frac{d}{dt}\int_{i-1/2}^{i+1/2} \boldsymbol{u}dx + \boldsymbol{f}_{i+1/2} - \boldsymbol{f}_{i-1/2} = \int_{i-1/2}^{i+1/2} \boldsymbol{s}dx \tag{3.3}$$

Eq. (3.3) is the statement of laws of mass and momentum conservation for the ith control volume. Let $\boldsymbol{U}_i$=mean value of $\boldsymbol{u}$ in the interval $[i-1/2, i+1/2]$. Eq. (3.3) becomes

$$\frac{d\boldsymbol{U}}{dt} = \frac{\boldsymbol{f}_{i-1/2} - \boldsymbol{f}_{i+1/2}}{\Delta x} + \frac{1}{\Delta x}\int_{i-1/2}^{i+1/2} \boldsymbol{s}dx \tag{3.4}$$

The fluxes at cell interfaces can be determined from the Godunov schemes that requires the exact solution of the Riemann problem. Godunov schemes are conservative, explicit, and efficient. The formulation of a Godunov scheme for the mass and momentum flux $\boldsymbol{f}_{i+1/2}$ in Eq. (3.4) for all i and for $t \in [t^n, t^{n+1}]$ requires the exact solution of the following Riemann problem[15]:

$$\frac{\partial \boldsymbol{u}}{\partial t} + \frac{\partial \boldsymbol{f}(\boldsymbol{u})}{\partial x} = 0 \quad \text{and} \quad \boldsymbol{u}^n(x) = \begin{cases} \boldsymbol{U}_L^n & for \quad x < x_{i+1/2} \\ \boldsymbol{U}_R^n & for \quad x > x_{i+1/2} \end{cases} \tag{3.5}$$

where $\boldsymbol{U}_L^n$ = average value of $\boldsymbol{u}$ to the left of interface i+1/2 at n; and $\boldsymbol{U}_R^n$ = average value of $\boldsymbol{u}$ to the right of interface i+1/2 at n. The exact solution of

Eq. (3.5) at $i+1/2$ for all internal nodes i and for $t \in [t^n, t^{n+1}]$ is as follows:

$$\boldsymbol{u}_{i+1/2}(t) = \begin{pmatrix} H_{i+1/2} \\ V_{i+1/2} \end{pmatrix} = \frac{1}{2} \begin{pmatrix} (H_L^n + H_R^n) + \frac{a}{g}(V_L^n - V_R^n) \\ (V_L^n + V_R^n) + \frac{g}{a}(H_L^n - H_R^n) \end{pmatrix} = \boldsymbol{B}\boldsymbol{U}_L^n + \boldsymbol{C}\boldsymbol{U}_R^n \quad (3.6)$$

where $\boldsymbol{B} = \frac{1}{2}\begin{pmatrix} 1 & a/g \\ g/a & 1 \end{pmatrix}$; and $\boldsymbol{C} = \frac{1}{2}\begin{pmatrix} 1 & -a/g \\ -g/a & 1 \end{pmatrix}$.

Using Eq. (3.6), the mass and momentum fluxes at $i+1/2$ for all internal nodes and for $t \in [t^n, t^{n+1}]$ are as follows:

$$\boldsymbol{f}_{i+1/2} = \overline{\boldsymbol{A}}_{i+1/2}\boldsymbol{u}_{i+1/2} = \overline{\boldsymbol{A}}_{i+1/2}\boldsymbol{B}\boldsymbol{U}_L^n + \overline{\boldsymbol{A}}_{i+1/2}\boldsymbol{C}\boldsymbol{U}_R^n \quad (3.7)$$

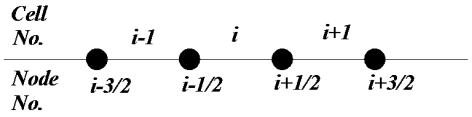

Fig. 3.1. Finite Volume grids system

The evaluation of the right-hand side of Eq. (3.7) requires that $\overline{\boldsymbol{A}}_{i+1/2}$, $\boldsymbol{U}_L^n$, and $\boldsymbol{U}_R^n$ are approximated. To estimate $\overline{\boldsymbol{A}}_{i+1/2}$, the entry associated with the advective terms, $\overline{V}_{i+1/2}$, needs to be approximated. Setting $\overline{V} = 0$ is equivalent to neglecting the advective terms from the governing equations. In general, an arithmetic mean be used to evaluate $\overline{V}_{i+1/2}$ [i.e., $\overline{V}_{i+1/2} = 0.5(V_i^n + V_{i+1}^n)$].

4 First-Order Godunov Scheme Formulation

The explicit evaluation of Eqs. (3.6) and (3.7) requires that $\boldsymbol{U}_L^n$ and $\boldsymbol{U}_R^n$ are written in terms of known nodal values. The first-order Godunov approximation is giving by[15]:

$$\boldsymbol{U}_R^n = \boldsymbol{U}_{i+1}^n \quad \text{and} \quad \boldsymbol{U}_L^n = \boldsymbol{U}_i^n \quad (4.1)$$

Inserting Eq. (4.1) into Eq. (3.7) completes the formulation of the first-order Godunov scheme:

$$f_{i+1/2} = \overline{A}_{i+1/2} B U_i^n + \overline{A}_{i+1/2} C U_{i+1}^n \tag{4.2}$$

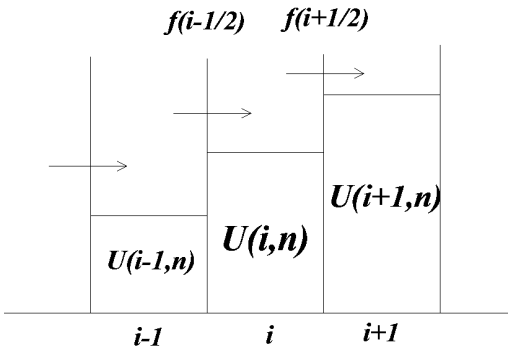

Fig.4.1. Finite Volume formulation

5 Second-Order Godunov Scheme Formulation

In general, the numerical dissipation in first-order scheme is more than in second-order scheme. Limiters increase the order of accuracy of a scheme while ensuring that results are free of spurious oscillations[15].

Using MINMOD limiter, an approximation for U_L^n and U_R^n that is second order in space and time is obtained as follows[15]:

$$\sigma_{j-1}^n = (U_j^n - U_{j-1}^n)/\Delta x \quad \text{and} \quad \sigma_j^n = (U_{j+1}^n - U_j^n)/\Delta x \tag{5.1}$$

$$MINMOD(\sigma_j^n, \sigma_{j-1}^n) = \begin{cases} \sigma_j^n & if \quad |\sigma_j^n| < |\sigma_{j-1}^n| \quad and \quad \sigma_j^n.\sigma_{j-1}^n > 0 \\ \sigma_{j-1}^n & if \quad |\sigma_j^n| > |\sigma_{j-1}^n| \quad and \quad \sigma_j^n.\sigma_{j-1}^n > 0 \\ 0 & if \quad \sigma_j^n.\sigma_{j-1}^n < 0 \end{cases} \tag{5.2}$$

$$U_{i-(1/2)^+}^n = U_i^n - 0.5\Delta x MINMOD(\sigma_j^n, \sigma_{j-1}^n) \tag{5.3}$$

$$U_{i-(1/2)^-}^n = U_i^n + 0.5\Delta x MINMOD(\sigma_j^n, \sigma_{j-1}^n) \tag{5.4}$$

$$U_{i+(1/2)^-}^{n^*} = U_{i+(1/2)^-}^n + \frac{1}{2}\frac{\Delta t}{\Delta x}[f(U_{i-(1/2)^+}^n) - f(U_{i+(1/2)^-}^n)] \tag{5.5}$$

$$\boldsymbol{U}^{n*}_{i-(1/2)^+} = \boldsymbol{U}^{n}_{i-(1/2)^+} + \frac{1}{2}\frac{\Delta t}{\Delta x}[\,\boldsymbol{f}(\boldsymbol{U}^{n}_{i-(1/2)^+}) - \boldsymbol{f}(\boldsymbol{U}^{n}_{i+(1/2)^-})] \tag{5.6}$$

$$\boldsymbol{U}^{n}_{R} = \boldsymbol{U}^{n*}_{i+(1/2)^+} \quad \text{and} \quad \boldsymbol{U}^{n}_{L} = \boldsymbol{U}^{n*}_{i+(1/2)^-} \tag{5.7}$$

Inserting Eq. (5.7) into Eq. (3.7) can give Godunov second-order scheme for the water hammer.

6 Boundary Conditions

The implementation of boundary conditions is a important step in solving partial differential equations. The boundary conditions in this model are:

6.1 Upstream Head-Constant Reservoir

The flux at an upstream boundary (i.e., i=1/2) can be determined from the Riemann solution. The Riemann invariant associated with the negative characteristic line is:

$$H_{1/2} - \frac{a}{g}V_{1/2} = H_1^n - \frac{a}{g}V_1^n \tag{6.1}$$

Coupling this Riemann invariant with a head-flow boundary relation determines[15]:

$$V_{1/2}^{n+1} = V_{1\frac{1}{2}}^{n} + \frac{g}{a}(H_{1/2} - H_{1\frac{1}{2}}^{n}) \tag{6.2}$$

For an upstream reservoir where $H_{1/2}^{n} = H_{res}$, the flux at the upstream boundary is:

$$\boldsymbol{f}_{1/2} = \begin{bmatrix} \overline{V}_{1/2}H_{res} + \dfrac{a^2}{g}(V_1^n + \dfrac{g}{a}(H_{res} - H_1^n)) \\ gH_{res} + \overline{V}_{1/2}(V_1^n + \dfrac{g}{a}(H_{res} - H_1^n)) \end{bmatrix} \tag{6.3}$$

6.2 Fully Closed Downstream valve

The flux at a downstream boundary can be determined from the Riemann solution. The Riemann invariant associated with the positive characteristic line is[15]:

$$H_{Nx+1/2} + \frac{a}{g} V_{Nx+1/2} = H^n_{Nx} + \frac{a}{g} V^n_{Nx} \tag{6.4}$$

Downstream boundary condition is valve closure in T_c . Head-flow boundary relation determines:

$$V^{n+1}_{Nx+1/2} = V_{steady}(1 - \frac{t}{T_c}) \qquad 0 \le t \le T_c \tag{6.5}$$

$$V^{n+1}_{Nx+1/2} = 0 \qquad t > T_c \tag{6.6}$$

$$H^n_{Nx+1/2} - H^n_{Nx-1/2} - \frac{a}{g}(V^{n+1}_{Nx+1/2} - V^n_{Nx-1/2}) = 0 \tag{6.7}$$

As a result, the flux at the boundary is determined as follows:

$$\boldsymbol{f}_{Nx+1/2} = \begin{bmatrix} \overline{V}_{Nx+1/2}(H_{Nx} + \frac{a}{g} V^n_{Nx} - \frac{a}{g} V_{Nx+1/2}) + \frac{a}{g} V_{Nx+1/2} \\ g(H_{Nx} + \frac{a}{g} V^n_{Nx} - \frac{a}{g} V_{Nx+1/2}) + \overline{V}_{Nx+1/2} V_{Nx+1/2} \end{bmatrix} \tag{6.8}$$

7 Time Integration

The previous section provided a first- and second-order scheme for the flux terms. In order to advance the solution from *n* to *n+1*, Eq. (3.4) needs to be integrated with respect to time. In the absence of friction, the time integration is exact and leads to the following:

$$\boldsymbol{U}^{n+1}_i = \boldsymbol{U}^n_i - \frac{\Delta x}{\Delta t}(\boldsymbol{f}^n_{i+1/2} - \boldsymbol{f}^n_{i-1/2}) \tag{7.1}$$

In the presence of friction, a second order Runge-Kutta solution is used and results in the following explicit procedure[15]:

$$\overline{\boldsymbol{U}}^{n+1}_i = \boldsymbol{U}^n_i - \frac{\Delta x}{\Delta t}(\boldsymbol{f}^n_{i+1/2} - \boldsymbol{f}^n_{i-1/2}) \tag{7.2}$$

$$\overline{\overline{\boldsymbol{U}}}_i^{n+1} = \overline{\boldsymbol{U}}_i^{n+1} + \frac{\Delta t}{2}\boldsymbol{s}(\overline{\boldsymbol{U}}_i^{n+1}) \tag{7.3}$$

$$\boldsymbol{U}_i^{n+1} = \overline{\boldsymbol{U}}_i^{n+1} + \Delta t.\boldsymbol{s}(\overline{\overline{\boldsymbol{U}}}_i^{n+1}) \tag{7.4}$$

8 Stability Condition

The time step should satisfy the Courant-friedrichs-Lewy (CFL) condition for the convective part:

$$Cr = \frac{a.\Delta t}{\Delta x} \le 1 \tag{8.1}$$

Although another stability condition should be used for the updating of a source term, it is found that the CFL condition is sufficient for the cases where the magnitude of the source term is small.

9 Friction in Water Hammer Flow

In this paper, the wall friction is modeled using the formula of Brunone et al. (1999)[15]:

$$J = \frac{fV|V|}{2D} + k(\frac{\partial V}{\partial t} - a\frac{\partial V}{\partial x}) \tag{9.1}$$

where D=pipe diameter; f = Darcy- Weisbach friction factor; k =unsteady friction factor; and a =wavespeed whose expression is as follows[9]:

$$a = \frac{\sqrt{K/\rho}}{\sqrt{1 + [(K/E)(D/e)]}} \tag{9.2}$$

where K=bulk modulus of elasticity of the fluid; E= Young's modulus of elasticity for the pipe; ρ =density of the fluid; and e =thickness of the pipe.

10 Numerical Results and Discussion

The objective of this section is to compare the accuracy and efficiency of Godunov scheme in solving water hammer problems. The MOC results and laboratory data are used for comparison.

10.1 Test Case I

Analytical solution data from Zhao and Ghidaoui(2004), and MOC results are used to investigate the accuracy of proposal model(Godunov scheme)[15]. The geometrical and hydraulic parameters for this test case are given in Table 10.1. This test case consists of a simple reservoir-pipe-valve configuration.

Table 10.1. Properties for the test case 1

Pipe diameter (m)	0.5
Pipe length (m)	1000
D.W friction factor	0.00
Unsteady friction factor	0.00
Wave speed(m/s)	1000
Reservoir head-upstream (m)	0
Initial mean velocity(m/s)	1.02
Cause of transients	Downstream instantaneous fully valve closure

Figure 10.1 shows the analytical and computed solutions for the variations in hydraulic head at the valve as a function of time.

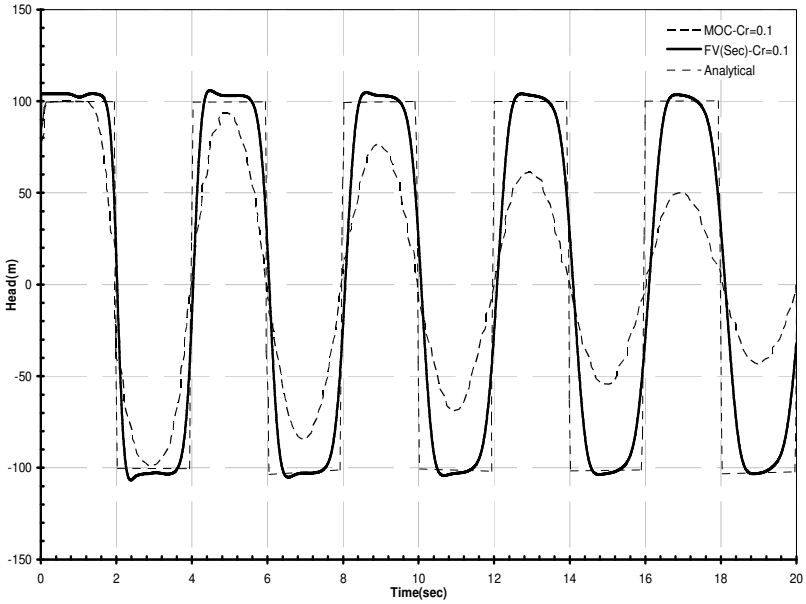

Fig.10.1. Variations in hydraulic head at the valve(Test 1) for MOC and FVM and analytical solution

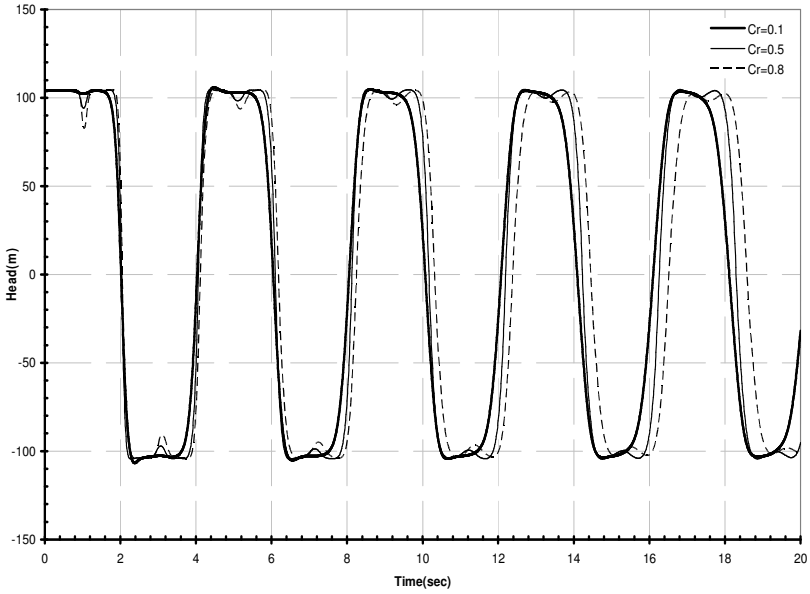

Fig.10.2. Pressure head traces at valve(Test 1) for various Cr(FVM)

As expected, the head traces results by both schemes (MOC and FVM) exhibit numerical dissipation, but the numerical dissipation in FVM is less than the MOC. In addition, the finite volume results affect by the Cr number. That is, the scheme reproduce the analytical solution when Cr=1.0 and for Courant number more less than one, the numerical dissipation of the scheme is more. Although the numerical dissipation in the Godunov scheme is less than other schemes. In addition, the grid size (mesh size) influences the results of the scheme.

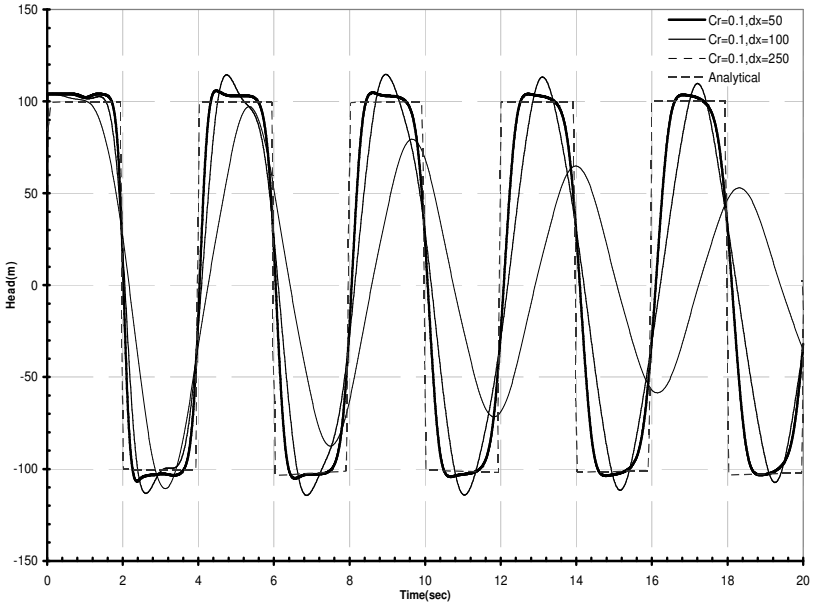

Fig.10.3. Pressure head trace at valve (test 1) for Cr=0.1 and different grid size (Finite Volume Method)

10.2 Test Case II

In this test case, laboratory data from Bergant and Simpson (1994) are used to investigate the accuracy of the FV scheme[10]. The geometric, kinematic, and dynamic parameters of this test are summarized in Table 10.2.

Table 10.2. Properties for the test case 2

Pipe diameter (m)	0.022
Pipe length (m)	37.20
D.W friction factor	0.034
Unsteady friction factor	0.00
Wave speed(m/s)	1319
Reservoir head-upstream (m)	32.0
Discharge(Lit/s)	0.114
Density(kg/m^3)	1000
Viscosity(m^2/s)	1.02
Cause of transients	Downstream valve closure in 0.009 seconds

Figure 10.4 shows the laboratory data and computed solutions (FVM and MOC) for the head value at the valve as a function of time. Figure 10.4 shows that both models accurately reproduce the time distribution of the experimental pressure wave, including its peak and phase, over the entire simulation time. In addition, the both models accurately capture the experimental pressure wave peak and phase, but the finite volume scheme produce a better fit for the entire pressure distribution than the MOC.

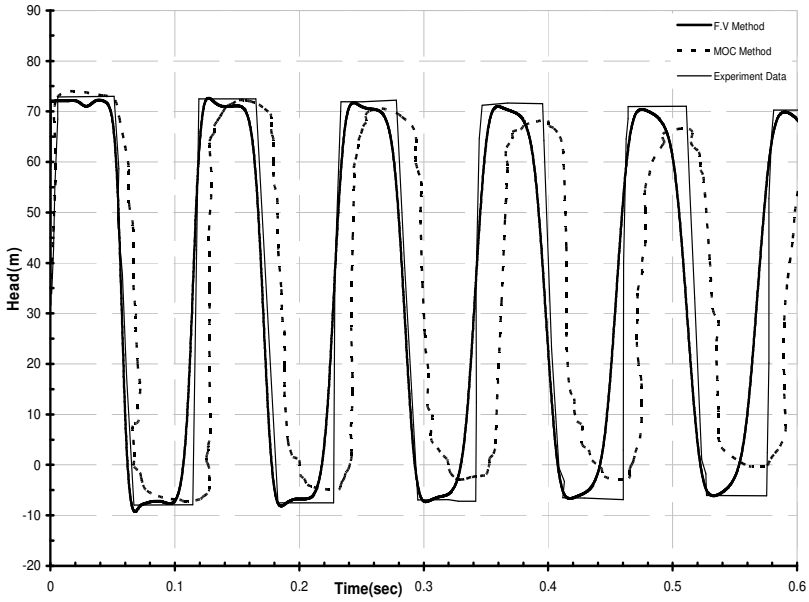

Fig.10.4. Variations in hydraulic head at the valve (Test 2) for MOC and FVM and laboratory data (Cr=0.5)

11 Conclusions

In this paper, second-order explicit finite volume Godunov-type scheme for water hammer problems are formulated, applied and analyzed. This scheme is compared with measured data from different research groups and with numerical data produced by a MOC model. The results are as follows.

1. Finite volume formulation conserves mass and momentum and produce physically realizable shock fronts.
2. The Godunov- type solution is stable for a Courant number less than or equal to one.
3. Nonlinear convective terms are included in governing equations.
4. Numerical dissipation in finite volume scheme is less than MOC and in close agreement with laboratory data.
5. The maximum and minimum of the pressure waves not only are computed in close agreement with experimental data, both also in the same period of time.
6. Similar to other numerical methods, finite volume results affected by computational grid size.

References

1. Ahmadi A, Chamani MR, Asghari K (2004) 1D Water Hammer Modeling by Finite Element Method for Complicated Boundary Conditions(in Farsi). M.Sc thesis, Isfahan University of Technology
2. Chaudhry M H (1979) Applied Hydraulic Transients. Van Nostrand Reinhold
3. Chung T J (2002) Computational Fluid Dynamics. Cambridge University Press
4. Enel-Cris M(2000) Hydraulic Transients with Water Column Separation. IAHR Secretariat
5. Guinot V (1998) Boundary Condition Treatment in 2×2 Systems of Propagation Equations. Int J Numer Meth Engng 42:647-666
6. Guinot V (2000) Riemann Solvers for Water-Hammer Simulations by Godunov Method. Int J Numer Meth Eng 49:851-870
7. Jovic V (1995) Finite Element and Method of Characteristics Applied to Water Hammer Modeling. Int J for Engng Modeling 8(3&4):21-28
8. Karney BW, Ghidaoui MS (1994) Equivalent Differential Equations in Fixed-Grid Characteristics Method. J Hydraul Eng 120(10):1159-1175
9. Larock BE, Jeppson RW, Watters GZ (1999) Hydraulics of Pipeline Systems. CRC Press
10. Ghidaoui MS, Mansour S (2002) Efficient Treatment of Vardy-Brown Unsteady Shear in Pipe Transients. J of Hydraul Engng 128(1):102-112
11. Mollabashi, A. (2002). Water Hammer Simulation by Finite Element Method. M.Sc Thesis(in Farsi), Isfahan University of Technology
12. Prado R A, Larreteguy AE (2002) A Transient Shear Stress Model for the Analysis of Laminar Water-Hammer Problems. J Hydraulic Researches 40: 45-53
13. Turani M (2004) Water Hammer Analysis With MOC For Karoun IV Penstocks(in Farsi). M.Sc thesis, K.N.Toosi University of Technology
14. Wylie EB, Streeter VL (1993) Fluid Transients in System. Prentice-Hall, Engle-wood, N.j
15. Zhao M, Ghidaoui MS (2004) Godunov-Type Solution for Water Hammer Flows. J of Hydraul Engng 130(4): 341-348